



THE UNIVERSITY *of* EDINBURGH

Edinburgh Research Explorer

Development of biodegradable nanogels for lipase accelerated drug release of 5-aminolevulinic acid

Citation for published version:

Liu, X, Zhang, Y, Zhang, P, Ge, K, Zhang, R, Sun, Y, Sheng, Y, Bradley, M & Zhang, R 2023, 'Development of biodegradable nanogels for lipase accelerated drug release of 5-aminolevulinic acid', *Colloids and Surfaces B: Biointerfaces*, vol. 225, 113268. <https://doi.org/10.1016/j.colsurfb.2023.113268>

Digital Object Identifier (DOI):

[10.1016/j.colsurfb.2023.113268](https://doi.org/10.1016/j.colsurfb.2023.113268)

Link:

[Link to publication record in Edinburgh Research Explorer](#)

Document Version:

Peer reviewed version

Published In:

Colloids and Surfaces B: Biointerfaces

General rights

Copyright for the publications made accessible via the Edinburgh Research Explorer is retained by the author(s) and / or other copyright owners and it is a condition of accessing these publications that users recognise and abide by the legal requirements associated with these rights.

Take down policy

The University of Edinburgh has made every reasonable effort to ensure that Edinburgh Research Explorer content complies with UK legislation. If you believe that the public display of this file breaches copyright please contact openaccess@ed.ac.uk providing details, and we will remove access to the work immediately and investigate your claim.



Development of Biodegradable Nanogels for Lipase Accelerated Drug Release of 5-Aminolevulinic Acid

Xiao Liu¹, Yuan Zhang¹, Peng Zhang^{1*}, Kang Ge², Ruzhi Zhang², Yixin Sun¹, Yang Sheng¹, Mark Bradley³ and Rong Zhang^{1*}

1. School of Materials Science and Engineering, Changzhou University, Changzhou 213164, Jiangsu, P. R. China

2. Department of Dermatology and Venereology, the Third Affiliated Hospital of Soochow University, Changzhou 213000, China

3. School of Chemistry, University of Edinburgh, Edinburgh EH9 3JJ, UK

* Corresponding author: Rong Zhang rzhang@cczu.edu.cn and Peng Zhang zp3033@126.com

Abstract: Photodynamic therapy (PDT) using 5-aminolevulinic acid (5-ALA) is an important approach for the treatment of some skin diseases and cancers. A major defect of this approach is that it is difficult for 5-ALA to accumulate around lesions in deeper regions of tissue, resulting in poor conversion to the active fluorophore and photodynamic efficiencies. Because of their targeting and controlled release abilities, nanogel carriers could solve this problem. In this paper, nanogels were prepared by using micro-emulsion polymerization with various biodegradable polyester crosslinkers (L-lactide and ϵ -caprolactone). The swelling and degradation properties and entrapment efficiency, drug loading and drug release ability of the nanogels were investigated. Nanogels co-cultured with skin cancer cells (A2058) allowed the efficiency of the PDT in vitro to be demonstrated. The results showed that the swelling rate of hydrogels reduced with increasing crosslinker levels, which caused a slow-down in the release of 5-ALA, but lipase accelerated degradation of nanogels increased 5-ALA concentrations in tumor cells and leading to higher PDT efficiency. It was proved by in vivo experiment indicating that the development of skin cancer tissues were efficiently inhibited by the 5-ALA loaded nanogels.

Key words: 5-ALA; photodynamic therapy; nanogels; biodegradable polyester crosslinker; controlled drug release

1. Introduction

Photodynamic therapy (PDT) based on 5-aminolevulinic acid (5-ALA) is an approach that allows (cancer) cells convert 5-ALA into protoporphyrin IX (PpIX) a photosensitizer (PS), which produces reactive oxygen species (ROS) upon exposing to specific wavelengths of light. Singlet oxygen (an oxygen molecule that can be considered to have a “+ve and -ve charge” and is hence exceptionally reactive will cause tumor cells to wither and inhibit their proliferation^[1]. ALA-PDT was endorsed for the clinic treatment of actinic keratosis^[2] and some skin diseases and cancers^[3].

As a second-generation PDT agent, 5-ALA is an excellent photosensitizer precursor as it is a hydrophilic small molecular weight compound, and a generic biosynthesis precursor of heme (on the pathway to hemoglobin). Thus, 5-ALA will be metabolized and transformed into PpIX under the action of a series of enzymes. Within healthy cells, PpIX is metabolised by ferrochelatase to heme. However, within tumour cells there is a reduced ferrochelatase expression resulting in both a build-up of PpIX which, due to lack of negative feedback, results in continual incorporation of 5-ALA into PpIX.

When illuminated at 405 nm PpIX is excited into an excited single state which undergoes inter-system-crossing to the triplet state. This reacts with oxygen to give rise to highly reactive singlet oxygen that will destroy cell membranes, mitochondria and other organelles and induce cell necrosis.

5-ALA has been widely used to treat skin diseases and several cancers on the surface of the tissue where irradiation is sufficient for PDT. It is however less efficient for tumor cells deep in tissue. Indeed, one of the problems of 5-ALA is its poor absorptive/localization capacity in tumor tissue, resulting in low efficiency of photodynamic response (exacerbated by the light scattering induced by tissue). Therefore, there are deficiencies in deep tumor treatment 5-ALA and PDT^[4, 5]. A promising method to help solve these problems is to use nano-carriers for 5-ALA delivery to increase its concentration in the tissues of a patient. Li et al ^[6] used

membrane fusion liposomes as carriers to encapsulate 5-ALA and combined this with iron to improve the photodynamic effect of 5-ALA, produced more singlet oxygen to promote the damage of tumor cells. However, liposomes have the disadvantage of poor structural stability because of easy oxidation and hydrolysis, and prone to aggregation or even liposome fusion, resulting in drug leakage^[7]. Nanosphere carriers made from polymeric materials loaded with drugs show excellent biocompatibilities, and can be targeted to specific tissues and organs and then slowly released their cargo. Nano capsules can be prepared with biodegradable and biocompatible polymers for drug delivery to increase local drug concentrations, changing their distribution and pharmacokinetic properties, ideally reducing toxicity to normal tissues^[8]. Shi et al^[9] enhanced the efficacy of PDT by encapsulation of 5-ALA within polylactic acid-*co*-glycolic acid nanoparticles (PLGANPs) that lead to the inhibition of human skin squamous carcinoma. However, it is difficult to achieve responsive drug release due to the uncontrollability of the release rate of 5-ALA from nano capsules. Nanogels are drug carriers with three-dimensional network structure that are water-based, have a stable structure and show good biocompatibility. Here we targeted nanogels to allow the responsive release of 5-ALA through the design of specific chain segments.

The expression of many enzymes is increased in cancer cells, with proteolytic enzymes, hyaluronidase, lipase, matrix metalloproteinase and various fibrinolytic enzyme^[10] all increased. Hou^[11] found that lipase was highly expressed in liver cancers (enhanced ester hydrolysis^[12]). Therefore, nanogels prepared with polyester crosslinkers would degrade more rapidly and release their cargoes more rapidly in cancer cells than that in normal cells. Polycaprolactone is a polyester and is a common scaffold material for tissue engineering, with good biocompatibility and mechanical properties, but it has poor hydrophilicity, readily crystallizes and has slow degradation^[13-15]. The crystallinity of polycaprolactone can be reduced by copolymerization with lactic acid^[16]. The hydrophilicity of the polyester can also be

increased by copolymerizing with polyethylene glycol as a chain segment, which also reduces the immunogenicity of large biomolecules, the clearance rate of kidney, and promotes the stability of nanogels^[17].

In this work poly (ϵ -caprolactone-co- L-lactide)-polyethylene glycol copolymer (PCLA) was prepared by ring-opening polymerization of ϵ -caprolactone (ϵ -CL) and L-lactide (L-LA) initiated by polyethylene glycol 1000 (PEG1000). A macromolecular crosslinker (PCLAMA) was prepared by capping PCLA with methacrylic anhydride, to endow it with lipase responsiveness and biocompatibility.

N-vinylpyrrolidone (NVP)^[18] and cationic monomer^[19] methacryloxyethyl trimethyl ammonium chloride (DMC), which could interact with the carboxylate of 5-ALA to promote encapsulating within the nanogels and promote endocytosis were used as monomers to prepare nanogels by microemulsion polymerization with PCLAMAs in different segment ratios as a crosslinker. The drug loading, swelling and degradation properties of the hydrogels and drug release profiles were studied. Skin cancer cells were co-cultured with the loaded nanogels to investigate their anti-cancer cell ability. The results were demonstrated by the in vivo experiments on animal models.

2. Materials and methods

2.1. Materials

5-ALA was purchased from McLean; Polyethylene glycol (M_w 1000) (PEG1000) was from Ling Feng Chemicals; ϵ -Caprolactone (ϵ -CL), L-lactide (L-LA), fluoramine, methacrylic anhydride, NVP and DMC were purchased from Aladdin; Dulbecco's modified eagle medium (DMEM) dry powder was purchased from Life Technologies, and fetal bovine serum was purchased from NQBB, the CCK-8 kit was from Abmole Bioscience. A2058 skin cancer cells were purchased from Jinyuan Biological; All chemicals were used as received.

2.2. Fluorescence labeling of 5-ALA

The fluorescence intensity of 5-ALA labeled with fluoramine (Fig. 1a) was measured by a transient fluorescence spectrometer (FIS1000, Tyco Shipu (Beijing) Technology) with λ_{ex} 398 nm and λ_{em} 480 nm. The concentration of 5-ALA solution was 0.005, 0.0025, 0.001, 0.00075 and 0.0005 mg/mL. The solutions were shaken and left to stand still for 30 min. The fluorescence intensity of the solution was measured by the fluorescence spectrophotometer and the standard concentration curve of 5-ALA was drawn.

2.3. Synthesis of macromolecular crosslinker

20 g PEG1000 was dried at 110 °C in vacuum for 2 hours. ϵ -CL and L-LA were added in proportion of PEG1000: ϵ -CL: L-LA= 1: 3.333: 1.667 or 1: 6.666: 3.333 or 1: 10: 5 followed with stannous octoate 8 wt%. The reaction was carried out in nitrogen for 24 hours at 130 °C. The mixture was cooled to room temperature and added with 12 mL chloroform before precipitating in a mixture of anhydrous ether and n-hexane (1:2). The precipitated prepolymer was purified by centrifugation and re-dissolving for 3 times to obtain prepolymer PCLA, which was dried in a vacuum oven at 50 °C for 24 h. The products of the three proportions were recorded as PCLA-5, PCLA-10 and PCLA-15 with the yields of 92%, 90% and 90% respectively.

10 g PCLA was dissolved in 40 mL dichloromethane in an ice-water bath. Triethylamine and methacrylic anhydride were dropped in the molar ratio of PCLA: methacrylic anhydride: triethylamine = 1:4:4. The mixture was stirred under nitrogen for 2 hours and then reacted at 30 °C for 48 h. After the reaction, the product was purified for 3 times by centrifuging precipitate in a mixture of anhydrous ether and n-hexane (1:2) and re-dissolving in dichloromethane. The product was then dried in a vacuum oven at 40 °C for 24 hours (Fig. 1b). The yields of PCLAMA-5, PCLAMA-10 and PCLAMA-15 were 83%, 84% and 87% respectively.

2.4. Preparation of biodegradable hydrogels

The hydrogels were prepared by dissolving PCLAMA (0.5 g), NVP and DMC in N-dimethylformamide (DMF, 1.8 mL), adding 8 wt% photoinitiator (I2959) and

stirred under nitrogen for 5 min before moving 600 μL of the mixture to the round PTFE mould (12 mm in diameter, 1 mm in depth) and irradiated under UV light (365 nm) for 60 min. The monomer ratios for preparing hydrogels are shown in Fig. 2a. The hydrogels were immersed in acetone and deionized water for 24 hours respectively followed with drying in a vacuum oven at 50 $^{\circ}\text{C}$ to a constant weight.

2.5. Preparation of biodegradable nanogels

0.5 g PCLAMA was weighed and mixed with NVP and DMC in the proportion (Fig. 2a) in 4 mL chloroform, and 8 wt% SDS in 120 mL deionized water. After adding the oil phase to the aqueous phase, the emulsion was stirred in high-speed (1500 r/min) for 1 h before exposing to UV light (365 nm) for 1 h. The flask was opened and then heated in an oil bath at 55 $^{\circ}\text{C}$ for 8 hours to remove chloroform from the emulsion. The obtained nanogel solution was dialyzed in deionized water for 48 hours, refreshing every 4 hours (the molecular-weight cutoff of the dialysis tube was 8-14 kDa). The dialyzed products were freeze-dried and stored in a desiccator for later use (Fig. S1).

2.6. Encapsulation of 5-ALA or FITC in nanogels

10 mg of the nanogels were suspended in 10 mL deionized water, dispersed by sonication, and then stirred with added 5-ALA in 5, 10, 15, 16.7, 20, 25, 30, 35 mg respectively for 48 h. The nanogels were separated by centrifugation (10000 r/min) to remove the liquid before freeze-dried and stored in a desiccator. The concentration of 5-ALA selected in the drug loading of nanogels was 1.67 mg/mL for all other experiments. FITC was loaded in the same way as above except that FITC was 10 mg.

2.7. Swelling ratio of hydrogels

The swelling ratio of hydrogel was characterized by volume analysis. The dried hydrogels (1 cm \times 1 cm \times 0.1 cm) was swelled in PBS (pH=7.4) for 24 hours at 37 $^{\circ}\text{C}$. The hydrogel samples were moved out, wiped with filter paper and measured the size of the swelled hydrogel with a vernier caliper for volume calculation, which was recorded as V_1 . The equilibrium swelling ratio was calculated according to the

following equation.

$$\text{Volumetric swelling ratio}(\%) = \frac{V_1}{1 \times 1 \times 0.1} \times 100\% \quad (1)$$

2.8. Degradation of hydrogels

The degradation of hydrogels was characterized by weight loss analysis. The dried hydrogel samples were incubated in PBS (pH=7.4, containing 1 mg/mL pancreatic lipase) and PBS (pH=7.4) respectively in a 24-well plate and oscillated in an air bath at 37 °C and 90 r/min. The hydrogel samples were removed from the degradation solution and washed with deionized water for 15 min at the designed time interval. The washed hydrogel samples were dried to constant weight in vacuum at 50 °C. The degradation rate of hydrogels was calculated by using equation 2.

$$\text{Weight loss}(\%) = \frac{W_0 - W_t}{W_0} \times 100\% \quad (2)$$

Here, W_t is the mass of a dried hydrogel sample after degradation at time t , mg; W_0 is the mass of a dried hydrogel sample before degradation, mg.

2.9. SEM analysis

Scanning electron microscopy (SEM, Hitachi Limited, Hitachi S4800) was used to analyze the morphology of nanogel microspheres before and after degradation and drug loading. The empty nanogels dispersed in deionized water were dropped on ethanol cleaned silicon wafers and dried to a constant weight in a blast drying oven at 45 °C. The samples were sprayed with gold before SEM analysis.

2.10. Particle size of nanogels

The particle size and its distribution of nanogels was measured by laser particle size analyzer (ZEN-3600, Malvern) under the condition of scattering angle 90°, wavelength 633 nm and temperature 25±0.1 °C. The nanogels were dispersed in deionized water, sonicated for 20 min and filtered twice with a 0.45 μm filter before

analyzing.

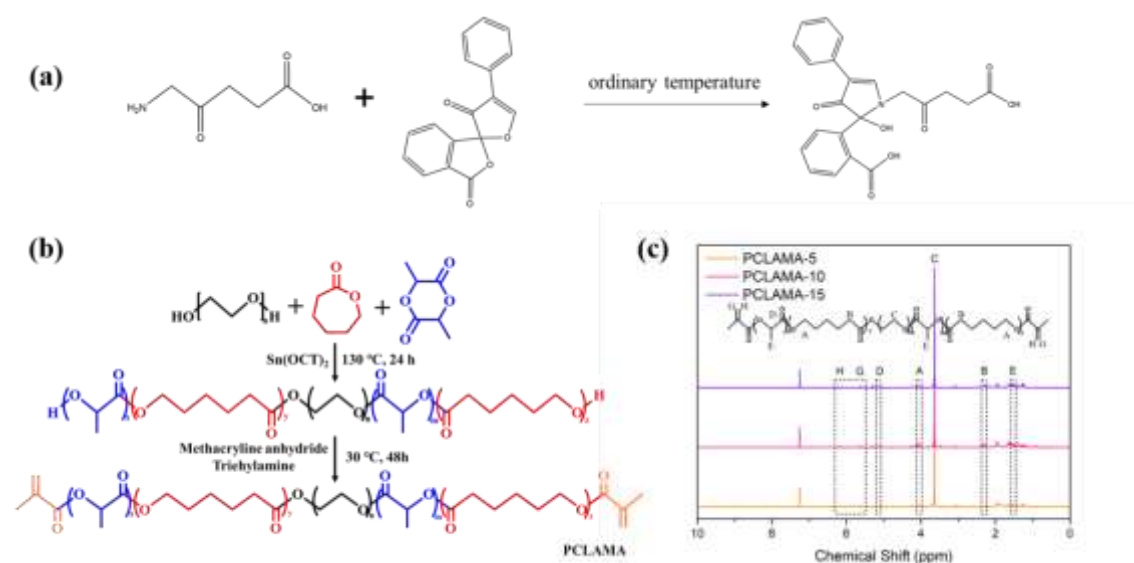


Figure 1 (a) The reaction of fluoramine with 5-ALA; (b) The synthesis of the macromolecular crosslinker PCLAMA; (c) ¹H-NMR spectra of PCLAMA-5, PCLAMA-10 and PCLAMA-15 with CDCl₃ as solvent (See Supporting Information).

2.11. Drug encapsulation efficiency and loading rate of nanogels

As drug encapsulation in nanogels described earlier, 2 mL supernatant were taken for fluoramine labeling after centrifugation. The fluorescence intensity of the supernatant was measured to find the concentration according to the standard concentration curve of 5-ALA for the calculation of the mass of 5-ALA in the supernatant (W_1). Therefore, the encapsulation efficiency and drug loading of nanogels were calculated according to the equations 3 and 4 respectively.

$$\text{Encapsulation efficiency}(\%) = \frac{W_0 - W_1}{W_0} \times 100\% \quad (3)$$

$$\text{Drug loading}(\%) = \frac{W_0 - W_1}{W_q + W_0 - W_1} \times 100\% \quad (4)$$

Here, W_1 is the mass of 5-ALA in the supernatant, mg; W_0 is the total mass of 5-ALA before drug loading, mg; W_q is the mass of nanogels, mg.

2.12. Drug release of nanogels

5 mL drug-loaded nanogels (0.15 mg/mL) with 5 mg pancreatic lipase and 5 mL drug-loaded nanogels were dialyzed in 15 mL PBS (pH=7.4, 1 mg/mL pancreatic lipase) and 15 mL PBS (pH=7.4) respectively in an air bath thermostat oscillator at 37 °C and 90 r/min. The molecular cutoff of the dialysis tubes was $M_w=8000-14000$. At each time point of 1 h, 2 h, 4 h, 7 h and 24 h during drug release, 2 mL solution was taken from the dialysis solution for the fluorescence measurement of 5-ALA after labeled with fluoramine. The dialysis solution was re-filled with 2 mL of the fresh PBS. The concentration of 5-ALA (C_n) in the dialysis solution was obtained by using the standard concentration curve of 5-ALA. The drug release rate of nanogels is calculated by the equation 5.

$$\text{Drug release rate}(\%) = \frac{C_n V + \sum_{i=0}^{n-1} C_i V'}{W_0} \quad (n = 1,2,3,4,5) \quad (5)$$

Here, C_n is the concentration of 5-ALA of the dialysis solution at a time point, mg/mL; V is the volume of the drug release medium ($V=15$ mL), mL; V' is the volume of the PBS solution containing 5-ALA ($V'=2$ mL), mL; W_0 is the total mass of 5-ALA loaded in nanogels, mg.

2.13. Co-culturing of nanogels with A2058 skin cancer cells

Nanogels (W10-2-COOH) with carboxyl group were prepared by adding acrylic acid monomer during polymerization. W10-2-COOH nanogels (100 mg) were dispersed in the solution of N, N-diisopropylcarbodiimide (DIC) and ethyl cyanoacetate-2-oxime (both in 2 eq. to acrylic acid in nanogels) in 5 mL of N, N-dimethylformamide (DMF) and stirred at 30 °C for 10 min before 4 equivalent of ethylenediamine added and stirred for 30 min. The nanogels with primary amine groups (W10-2-NH₂) were collected by centrifugation (10000 r/min) and washed with DMF for three times. Then FITC or activated rhodamine-B (2 eq.) was added into DMF (5 mL) with dispersed W10-2-NH₂ and stirred at 30 °C for 30 min before

centrifugation (10000 r/min) and washing with DMF for three times. At last, the W10-2 nanogels conjugated with fluorophores (W10-2FITC/RhB) were washed with distilled water until the supernatant became transparent without color (checked with UV/vis spectrometer). The W10-2FITC/RhB nanogels were used to trace the endocytosis of the nanogels by A2058 skin cancer cells. The W10-2FITC/RhB nanogels were dispersed in complemented H-DMEM at a concentration of 0.13 mg/mL. The media with nanogels were filtered through 0.45 μ m filters and added to a 6-well plate with 80% confluent A2058 cells (2 mL/well) and cultured in an incubator at 37 °C with 5% CO₂ for 4 hours. The culture medium was removed and the cells were washed with PBS for 3 times before fixing with 0.5 mL paraformaldehyde (4%) per well at room temperature for 15 min. The cells were washed with PBS 3 times before stained with 0.5 mL DAPI solution (10 μ g/mL) per well for 10 min at room temperature. The cells were washed with PBS for 3 times and imaged with a fluorescence microscope.

2.14. The dynamics of PpIX production in cells

The level of PpIX produced was characterized using a fluorospectrophotometer looking at the fluorescence intensity of PpIX produced in the cells. The experiment samples included five groups: cells cultured with 0 mM 5-ALA, 1 mM 5-ALA, 2 mM 5-ALA, 0.13 mg/mL W10-2 (1 mM 5-ALA) and 0.13 mg/mL empty W10-2 without 5-ALA respectively. Each group had three repeats. Nanogels of each group were added in 1 mL per well to a 12-well plate inoculated with 5×10^5 A2058 cells per well. The culture medium was removed at 2 h, 4 h, 6 h, 10 h and 24 h respectively, and the cells were washed with PBS for 3 times. The cells were lysated by RIPA lysis buffer to extract the PpIX produced in the cells and then 2 mL of water was added to each well before measuring on a fluorescence spectrophotometer (λ_{ex} :410 nm, λ_{em} :630 nm).

2.15. Photodynamic effect of nanogels on A2058 cells

The culture media with drug or nanogels were prepared with different concentrations of 5-ALA, 0 mM, 1 mM, 2 mM, 0.13 mg/mL W10-2 (1 mM 5-ALA)

and 0.13 mg/mL W10-2 without 5-ALA. The drug media were added to the 96-well plate with 80% confluent A2058 cells in 100 μ L/well (each group having three repeats). The wells were irradiated with 635 nm light from an integrated LED lamp board (power: 10 mW/cm²) for 10 min after culturing for 8 h or 24 h, and continued to culture for 24 h. The cellular viability was analyzed with a CCK-8 assay. In details, the culture media was removed from the 96 well plate and the cells were washed with PBS for three times before adding 100 μ L H-DMEM containing 10% CCK-8 in each well. The cells were cultured for 4 h (37 °C with 5% CO₂) before analysis on a plate reader at 450 nm. The cell viability was calculated following equation 6.

$$\text{Cell viability (\%)} = \frac{A_1 - A_b}{A_0 - A_b} \times 100\% \quad (6)$$

Here, A_1 is the absorbance of the cell group cultured with nanogels, A_b is the absorbance of the complemented L-DMEM without cells and A_0 is the absorbance of the cell group without culturing with nanogels.

2.16. Photodynamic effect of 5-ALA on A2058 cells/ fibroblasts

The media with various concentrations of 5-ALA (1 mM, 2 mM, 3 mM, 4 mM and 5 mM) were used for culture of A2058 cells or fibroblasts for 8 h and 24 h before exposed to 635 nm light for 10 minutes. CCK-8 assay was carried out for analyzing cell viability after 24 hours of culture.

2.17. Live / dead assay

The media (100 μ L/well) contained 0.13 mg/mL of W10-2 (1 mM 5-ALA) and was added to the 96-well plate with 80% confluent A2058 cells, with the cells cultured without drug as a control. The cells were irradiated with 635 nm light for 10 min after 8 h or 24 h culture. The cells were cultured for another 24 h before removing the culture medium and washed with PBS for 3 times. 100 μ L of PBS of Calcein AM and propidium iodide (both 0.1 wt% in PBS) were added to each well for cellular immunofluorescence staining. The cells were washed 3 times and imaged.

2.18. Flow cytometry

The culture medium (1 mL/well) containing 1 mM 5-ALA and 0.13 mg/mL of W10-2 (1 mM 5-ALA) was added to the 12-well plate with 80% confluent A2058 cells and incubated for 8 h or 24 h in an incubator at 37 °C with 5% CO₂ before irradiated with 635 nm light for 10 min, with the cells without drug as controls. The cells were cultured for another 24 h before detached with trypsin. The cells were centrifuged at 1500 r/min for 5 min and washed with PBS for three times. The cells were then stained with 1 mL propidium iodide solution in PBS (4.5 μM, from Solarbio) at room temperature for 5 min before washed with PBS for 3 times and dispersed in PBS in 2×10⁵ cells/mL for flow cytometry analysis.

2.19. In vivo photodynamic effect of nanogels

Murine melanoma cells (B16F10, 2×10⁶ cells/mL) were injected subcutaneously into female KM mice (Nanjing Qing Long Mountain Breeding Base, Jiangsu, China) to establish tumor bearing mice model. When the average tumor volume reached 30-50 mm³, the mice were randomly divided into four groups (n =6/group) for treatment with PBS, 5-ALA, W10-2(1mM 5-ALA) and W10-2 respectively (5-ALA dose: 50 mg/kg; W10-2 dose: 30 mg/kg) by peritumoral injection on day 1, 3, 5 and the tumor tissues on mice were exposed to 635 nm light for 10 min (power: 10 mW/cm²) on day 2, 4 and 6. The amount of free 5-ALA was equivalent to the amount of 5-ALA loaded in W10-2 in each injection dosage. The tumor volume (mm³) and the tumor growth inhibition value (%) were calculated by equation 7 and 8 respectively.

$$\text{Tumor volume} = \text{tumor width}^2 \times \text{tumor length} \times 0.5 \quad (7).$$

$$\text{The tumor growth inhibition value (\%)} = (1 - \text{RTV}/\text{RTV}_0) \times 100\% \quad (8)$$

Here, RTV₀ is the average tumor volume of the mice group treated with PBS; RTV is the average tumor volume of the mice group treated with other drugs.

Tumor growth and body weight were measured every day. The mice were sacrificed and the tumor tissues were collected after 12 days.

2.20. Statistical analysis

Statistical analysis was performed using the software Origin for the calculation of the p value. A value of $*p < 0.05$ was considered statistically significant. All data were expressed as mean values \pm standard deviation.

3. Results and discussion

3.1. Preparation and Characterization of PCLAMA and its hydrogels

Poly(ϵ -caprolactone-co-L-lactide)-polyethylene glycol dimethacrylate (PCLAMA) was synthesized by ring-opening polymerization and capped with methacrylic anhydride. The PEG-1000/ ϵ -CL/L-LA ratios were: 1: 3.33: 1.67 or 1: 6.67: 3.33 or 1:10:5 and recorded as PCLA-5, PCLA-10 and PCLA-15. They were converted to crosslinkers PCLAMA-5, PCLAMA-10 and PCLAMA-15 (Fig. 1b). The synthesized PCLAMA were characterized with $^1\text{H-NMR}$, FTIR and GPC (Fig. 1c, S2 and Table S1). The molecular weight of the PCLAMA's (as analyzed by GPC) gave M_n of 2300, 2800 and 3700 Da (Table S1), slightly larger than the theoretical M_n of the three crosslinkers (1620, 2241 and 2861 Da) presumably due to the polystyrene standards used on the GPC. The results indicated that the PCLAMAs were successfully prepared.

The hydrogels were prepared using a mixture of PCLAMA with NVP and DMC with the monomer ratios shown in Fig. 2a. The swelling ratio and degradation properties were characterized using hydrogel pieces made by UV initiated polymerization in a mould with the dimension of 12 mm in diameter and 1 mm in depth. The nanogels were prepared by emulsion polymerization. The particles size, drug loading and release, photodynamic activities were carried out using nanogels and the results were compared for choosing the best nanogels for PDT on cancer cells.

It was reported that the volume swelling ratio (VSR) could better represent the pore size of hydrogel^[20]. Therefore, the VSR of hydrogel was used here (Fig. 2b). The maximum VSR of K10-1 was 1092% due to the pore size of K10-1 being the largest among the hydrogels (Fig. S3, Table S2). Hydrogel K5-1 showed the smallest

swelling ratio because the PCLAMA-5 crosslinker was the shortest among PCLAMAs (Table S1) with a swelling ratio of 300%. The swelling ratio of hydrogel K15-1 was 782% although it had the longest polyester chain segment (PCLAMA-15). It also showed increased hydrophobicity. With the increasing of the amount of the crosslinker, the volume swelling ratio of hydrogel K10-1 reduced from 1092%, to 413% and 286% because of increased crosslinking levels. Therefore, it is possible to control the release of 5-ALA loaded nanogels by tuning the crosslinker level during hydrogel preparation with low molecular weight or hydrophobic crosslinkers or increasing the amount of crosslinkers. Under these conditions, the mass swelling rate of the hydrogels showed the similar trend (Fig. S4).

It was found that the degradation of hydrogels in the buffer with enzyme was faster than that with just PBS (Fig. 2c, d). The degradation rate of K10-1 reached 71% in 8 days with enzyme, and 57% in PBS. The degradation rates of K5-1 and K15-1 were slightly lower than that of K10-1 (43% and 45% respectively). The trend agreed with the results of the swelling ratios of the five hydrogels. The degradation rate of K10-2 and K10-3 was less than 25% under both conditions after 8 days, because the crosslinking degree of the hydrogels increased. Therefore, 5-ALA could be released more gradually from K10-2 or K10-3 than any other hydrogels.

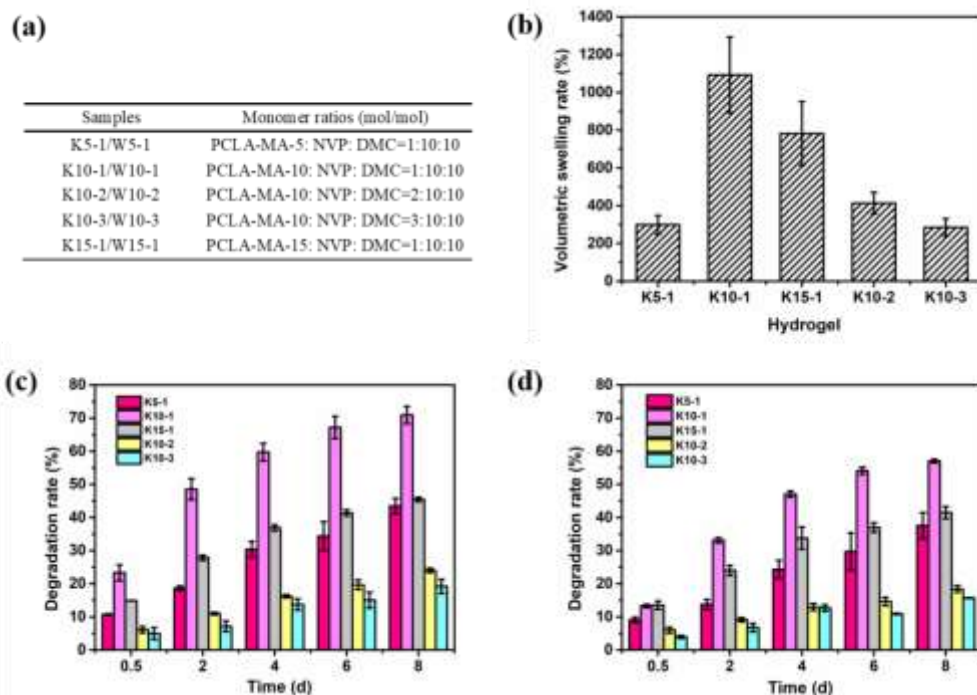


Figure 2 Characterization of hydrogels crosslinked with PCLAMAs. (a) Table of monomer ratios of hydrogels with various PCLAMA crosslinkers. K stands for bulk hydrogel; W stands for nanogel; NVP - N-vinylpyrrolidone and DMC - methacryloxyethyl trimethyl ammonium chloride. (b) The volume swelling ratios of the fabricated hydrogels in PBS (pH=7.4); (c) Degradation rates of hydrogels in PBS (pH=7.4) with 1 mg/mL pancreatic lipase and (d) degradation rates of hydrogels in PBS (pH=7.4) (n=3). The error is STDEV.

3.2. Particle size analysis of nanogels

The average particle sizes of the nanogel W10-1, W15-1 and W10-2 were 108 nm, 126 nm and 278 nm respectively according to DLS analysis (Fig. 3a,b,c). The particle sizes of W5-1 and W10-3 were uneven with two or more peaks with some large particles (Fig. S5). Therefore, W10-2 was further studied in this work. The particle size and zeta potential of W10-2 in PBS, PBS+10% FBS and normal saline were analyzed (Fig. S6). The zeta potential of W10-2 remained stable within 15 days. The particle size of W10-2 increased dramatically in the first 1-2 days and remained stable after reaching swelling equilibrium. The morphology of the W10-2 nanogels

was analyzed with TEM. The TEM images of W10-2 nanogels, W10-2 loaded with 5-ALA and W10-2 treated with pancreatic lipase were shown in Fig. 3d, e and f. The results showed that the empty nanogels were spherical with an average particle size of 170 nm, somewhat smaller than that measured by light scattering due to the dry state needed for TEM analysis (Fig. 3d). The average particle size (220 nm) of nanogels encapsulated with 5-ALA was bigger than the empty ones (Fig. 3e), possibly because of drug loading. The particle sizes of some degraded nanogels were much bigger with the particles size of some nanogels around 1 μm (Fig. 3f). The possible reason was that the degree of crosslinking in the nanogels reduced due to degradation, leading to greater swelling ratios. Some of small irregular broken nanogel pieces were also observed on the TEM image (Fig. 3f).

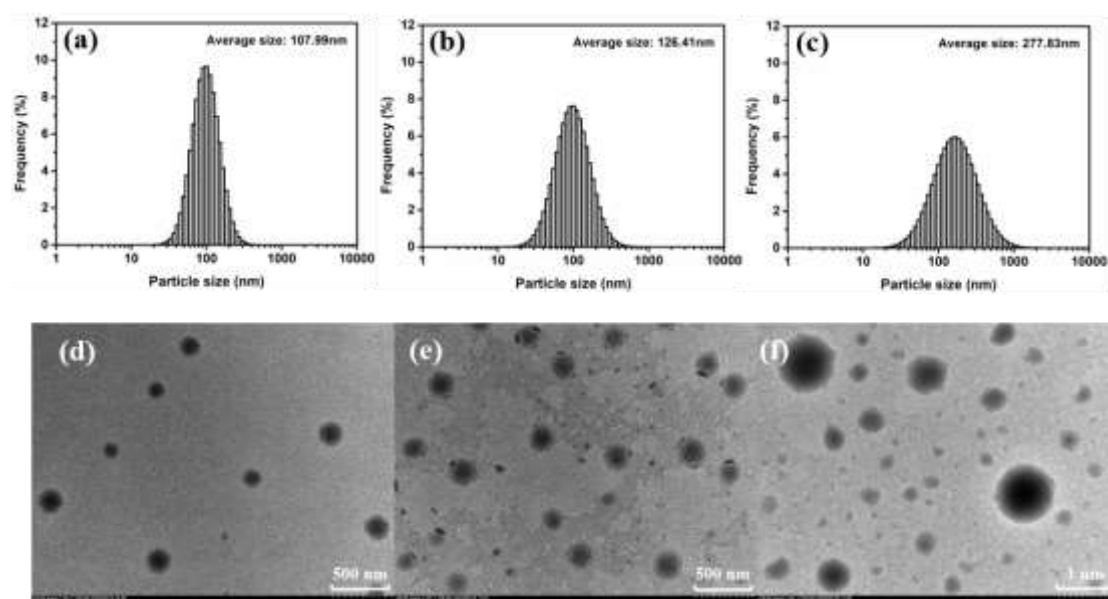


Figure 3 Particle characterization of nanogels. Particle size distribution of the nanogels (a) W10-1, (b) W15-1 and (c) W10-2 measured by DLS; TEM images of (d) nanogels of W10-2 without 5-ALA, (e) nanogels loaded with 5-ALA and (f) nanogels degrading in PBS (pH=7.4) with 1 mg/mL pancreatic lipase for 8 h.

3.3. Drug loading and release of 5-ALA

The encapsulation efficiencies of 5-ALA in W10-1, W15-1 and W10-2 were 76.13%, 72.95% and 72.40% and the 5-ALA loading was 56%, 55% and 55%

respectively (Fig. 4a, b), which were high comparing to other carriers, such as chitosan and liposome^[21-23]. The reason for the high drug loading ability was possibly the interaction between the cationic monomer DMC in the gel and the negative charges on 5-ALA. In addition, the encapsulation efficiency and drug loading of nanogels with various 5-ALA concentrations (0.5, 1.0, 1.5, 2.0, 2.5, 3.0, 3.5 mg/mL) were also investigated (Fig. S7). It showed that when the concentration of 5-ALA was greater than 1.5 mg/mL, the encapsulation capacity of nanogels tended to be saturated. Therefore, 1.67 mg/mL of 5-ALA was used for drug loading of nanogels in the following experiments.

A standard fluorescent intensity curve of 5-ALA labeled with fluoramine was used for drug release analysis of nanogels (Fig. S8). The drug-loaded nanogels were in the stage of "initial burst release" in the first hour, releasing 5-ALA rapidly, which was probably the 5-ALA adsorbed on the surface of the nanogels (Fig. 4c, d). In the PBS (pH=7.4), the drug release rate of W10-1, W15-1 and W10-2 was 50.19%, 44.90% and 40.02% respectively after 24 h's release. The release of 5-ALA was mainly dominated by the swelling capacity of the gels. 5-ALA in W10-1 released more rapidly into the medium than any other gels, due to the highest swelling ratio and pore size of W10-1 among them (Fig. S3, Table S2). The release rate of W10-1, W15-1 and W10-2 in PBS (pH=7.4) with 1 mg/mL pancreatic lipase was 73.25%, 79.33% and 84.86% respectively after 24 h's release, faster than that in normal PBS, indicating that lipase caused degradation of nanogels and accelerated the release of 5-ALA from the nanogels.

It was found that W10-2 showed interesting drug release properties. When nanogels loaded with 5-ALA were in the PBS solution, the drug release rate of W10-2 was the lowest among the three nanogels. While the drug release rate of W10-2 reached the highest as the nanogels were in the PBS (pH=7.4) with 1 mg/mL pancreatic lipase (Fig. 4c, d). Therefore, the drug release behavior of W10-2 could response to the presence of lipase. When there wasn't lipase in the culture medium,

the drug release rate of W10-2 was less than 40% after 24 h's culture. More loaded drug was remained in the W10-2 nanogels. When W10-2 was suspended in the medium with lipase, the drug release rate increased to over 80% after 24 h's culture. Thus, W10-2 nanogels could be used for controlled drug delivery into cells due to much higher enzyme concentration in the cells than that out of cells.

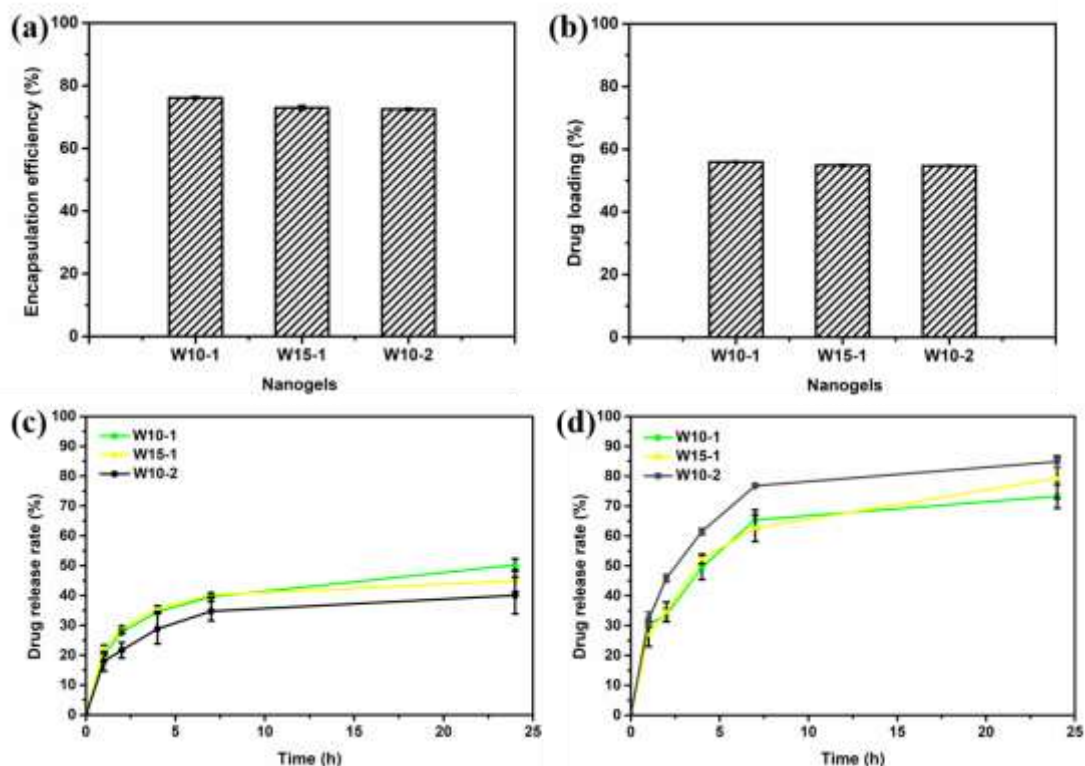


Figure 4 5-ALA loading and releasing of the nanogels. (a) Encapsulation efficiency of the nanogels; (b) Loading of 5-ALA in the nanogels; (c) The release rates of nanogels in PBS (pH=7.4) and (d) the release rates of nanogels in PBS (pH=7.4) with 1 mg/mL pancreatic lipase (n=3). The error is STDEV

3.4. Cellular uptake of nanogels and detection of cellular PpIX

It was found that the cell viability of human adipose-derived stem cells (hADSCs) and fibroblast after co-culturing with nanogels (W10-2) was over 100% and 95% when the nanogels were applied at 0.1 mg/mL, respectively (Fig. S9). The viability was about 80% at 0.15 mg/mL. Therefore, the nanogels of W10-2 were applicable at

0.15 mg/mL or less.

In order to find out if the nanogels can deliver the loaded cargo into cells, skin cancer cells (A2058 cells) were co-cultured with nanogels loaded with FITC for 4 hours, and then stained with DAPI^[22]. The cells were scanned layer by layer with two microns in step width by a confocal fluorescent microscope (Fig. 5a). At the first scanning (0 μm), the image showed the blue nucleus and green nanogels containing FITC in the cytoplasm. The blue nucleus gradually disappeared and the green fluorescence vanished too according to the images of other scanning layers, which indicated that the nanogels should enter the cells and located on the same level as the nucleus. From the fluorescent images, there were a large number of red particles aggregated in the cytoplasm around the blue nucleus after co-culturing with W10-2RhD nanogels (Fig. 5b). While some of green particles (W10-2FITC) were also observed in the cells (Fig. S10). This shows that the W10-2 nanogels entered the cytoplasm of the A2058 cells confirming that the nanogels delivered loaded cargo.

The more PpIX accumulated in cells, the more ROS produced after illumination, which affects the inhibition effect of PDT on cancer cells^[24]. The fluorescence intensity of protoporphyrin produced by A2058 cells due to 5-ALA inside the cells was analysed after co-culturing with drug carriers for 2 h, 4 h, 6 h, 10 h and 24 h (Fig. 5c). The results showed that the fluorescence intensity of PpIX in the cells without added 5-ALA (0 mM 5-ALA and empty W10-2 groups) was very low and did not increase with time, indicating that the cells did not generate PpIX. It was found that the fluorescent intensity was very similar for the cells cultured with 1 or 2 mM 5-ALA and nanogels (W10-2) loaded with 5-ALA (1 mM). However, the fluorescent intensity of W10-2 (1mM 5-ALA) group became higher than the 1 mM 5-ALA group after 24 hour's culture.

By studying the PDT effect of different concentrations of 5-ALA on A2058 cells or fibroblasts, it was found that 5-ALA was more toxic to cancer cells (Fig. 5d, e). The PpIX converted from 5-ALA in fibroblasts was rapidly converted into heme by

ferrous chelatase, which greatly reduces the effect of PDT. The lack of ferrous chelatase in cancer cells leads to a large accumulation of PpIX^[25]. When the concentration of 5-ALA was greater than or equal to 2 mM, the PDT effect reached equilibrium, which agreed to the published research results^[26].

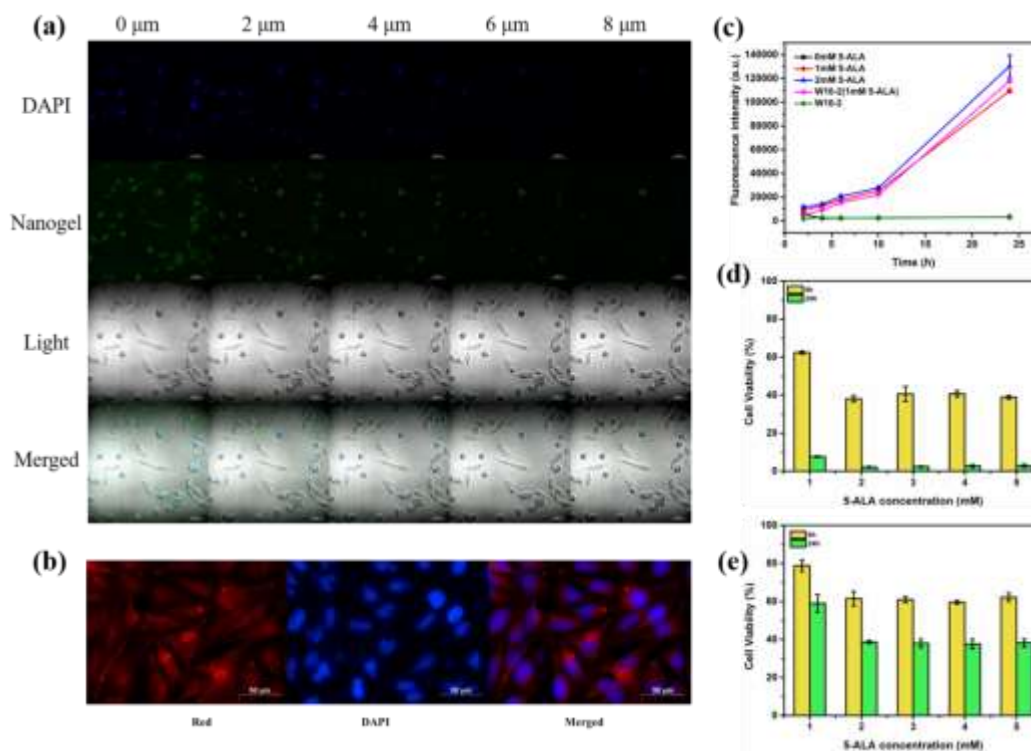


Figure 5 (a) Confocal microscope images of A2058 cells after co-cultured for 4 h with nanogels (W10-2, 0.1 mg/mL) loaded with FITC. The nucleus was stained with DAPI. Microscope filters: λ_{ex} =408 nm and 488 nm; (b) Fluorescence images of A2058 cells after co-cultured for 4 h with nanogels (W10-2, 0.1 mg/mL) grafted with rhodamine-B. The nucleus was stained with DAPI. Microscope filters: λ_{ex} =455 nm and 590 nm; (c) Fluorescence intensity of PpIX inside A2058 cells after cultured in media containing 0 mM, 1 mM or 2 mM 5-ALA or W10-2 nanogels (1 mM 5-ALA) and empty W10-2 nanogels over time (λ_{ex} :410 nm and λ_{em} :630 nm). Cell viability of (d) A2058 cells and (e) fibroblasts was analyzed by CCK-8 after co-culture with various concentrations of 5-ALA for 8 and 24 hours followed with 635 nm light illumination for 10 min.

3.5. Photodynamic effect on A2058 cells

A2058 cells were cultured in media with 5-ALA or nanogels loaded with 5-ALA for 8 h or 24 h, and then exposed to 635 nm light for 10 min followed by further culture for 24 h. The cell viability was analyzed and showed that there was no cytotoxicity for the media with 5-ALA or nanogels in the dark. For the cells cultured for 8 hours followed with 10 min illumination, cell viability with W10-2 (1 mM 5-ALA) was 30%. Cell viability with 1 mM 5-ALA was 67% (2 mM 45%), indicating that the 5-ALA encapsulated in W10-2 delivered better PDT activity than free 5-ALA (Fig. 6a). After 24 h culture and light illumination, cell viabilities of 1 mM or 2 mM 5-ALA and W10-2 (1 mM 5-ALA) were 4%, 0.9% and 1% respectively. Empty W10-2 nanogels showed no cytotoxicity after illumination (Fig. 6b). Thus, W10-2 nanogels loaded with 5-ALA were more efficient than 1 mM free 5-ALA presumably due to more direct cell delivery/perpetuation of delivery inside the cells. Under the same condition, the viability of fibroblasts was higher than that of A2058 cells after the PDT treatment of 5-ALA loaded nanogels (Fig. S11).

A2058 cells were cultured with and without W10-2 nanogels (1 mM 5-ALA) for 8 h or 24 h, and then illuminated at 635 nm (power: 10mW/cm²) for 10 min before further culture for 24 h and staining. The cytotoxicity of 0 mM 5-ALA, 1 mM 5-ALA and W10-2 (with 1 mM 5-ALA) on cells was analyzed by flow cytometry (Fig. 6c). The apoptosis rates of cells were 17.9%, 58.9% and 73.9% respectively after 8 h co-culture. With the increasing of the culture time to 24 h, the apoptosis rates became 15.9%, 94.9% and 93.7% respectively. Fluorescent images showed that the cells were viable when no 5-ALA or nanogels were added to the culture media (Fig. 6d). When cells were cultured with nanogels W10-2 loaded with 5-ALA for 8 h or 24 h and irradiated with light, the number of cells with a perturbed/damaged membrane increased (red cell pieces).

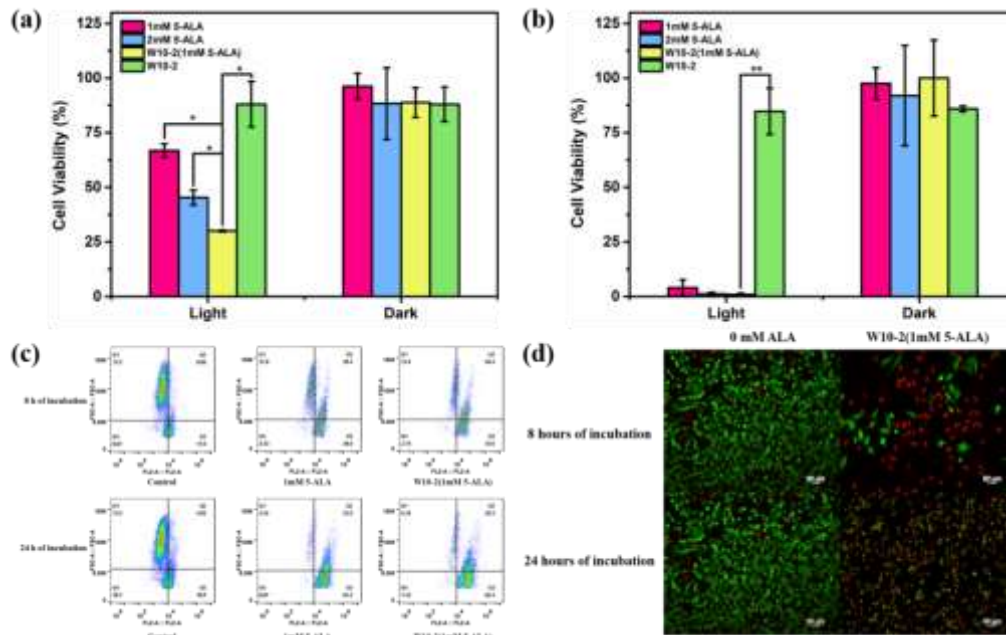


Figure 6 Cell viability of A2058 cells after cultured in media containing 1 mM 5-ALA, 2 mM 5-ALA, W10-2 loaded with 5-ALA (1mM) and empty W10-2 nanogels respectively for (a) 8 h or (b) 24 h before 10 min light illumination (635 nm) (* : $P \leq 0.05$; ** : $P \leq 0.01$); (c) Flow cytometry of A2058 cells stained with PI solution after 8 h and 24 h treatment with W10-2 nanogels (0.13 mg/mL) and illumination at 635 nm for 10 mins and 24 h incubation; (d) Fluorescent images of A2058 cells stained with a solution of Calcein AM and PI after 8 h and 24 h treatment with W10-2 nanogels (0.13 mg/mL) and illumination at 635 nm for 10 mins and 24 h incubation. Microscope filters: $\lambda_{ex} = 515$ nm and 590 nm. Scale bar = 50 μ m.

3.6. *In vivo* photodynamic effect of nanogels

The encouraging results of *in vitro* photodynamic experiment prompted us to further study the anti-tumor effect *in vivo*. The treatment design is illustrated in Fig. 7a. Briefly, when tumor volume reached 30-50 mm³, animals were administered with PBS, 5-ALA, W10-2(1mM 5-ALA) and W10-2 respectively by peritumoral injection and tumor tissues were irradiated by 635 nm laser lamp with power of 10 mW/cm² after 24 hours, which were carried out in the same way every day in the first 6 days. All animals were euthanized on day 12. The relative tumor volume of mice treated

with W10-2 (1mM 5-ALA) was smaller than that of free drug, indicating that W10-2 nanogels loaded with 5-ALA could inhibit tumor growth much better in vivo (Fig. 7b). The tumor growth inhibition value of the animal group treated with drug loaded nanogels and that with free 5-ALA were 93.18% and 48.83% respectively. During the treatment, all animals were survived and their body weight increased gradually in the similar trend, which indicated that the photodynamic treatment strategy was safe (Fig. 7c, d). However, the size and mass of the tumor tissues in mice treated with 5-ALA loaded nanogels were much smaller than that of free 5-ALA (Fig. 7e, f). This shows that 5-ALA loaded W10-2 nanogels could significantly improve the inhibition of tumor development in vivo and had no obvious toxic and side effects.

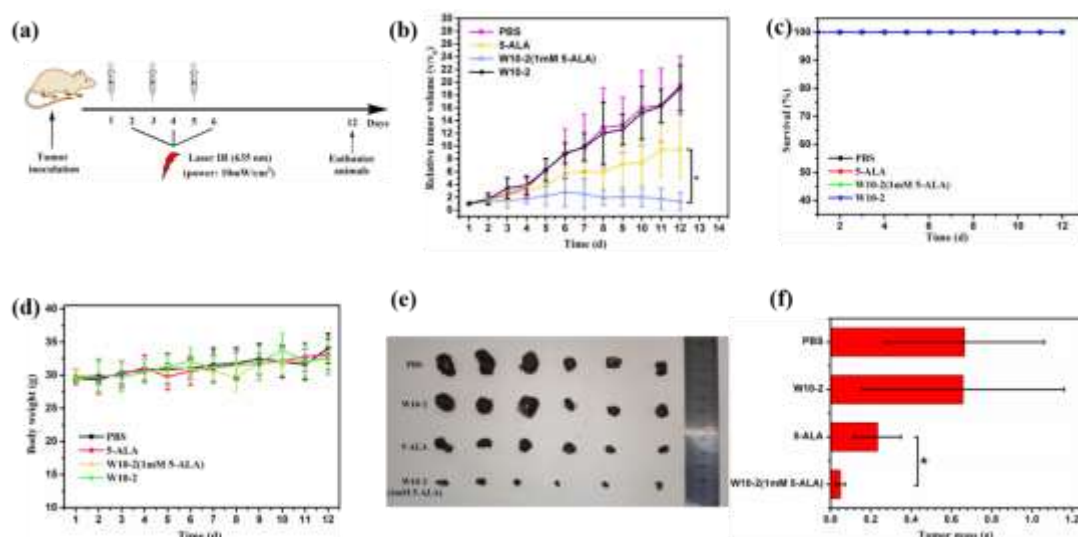


Figure 7 The results of in vivo photodynamic treatment on KM mice. (a) The treatment protocol for B16F10 tumor-bearing mice; (b) Tumor volume of mice treated with PBS, 5-ALA, W10-2 (1mM 5-ALA) and empty W10-2 respectively (n=6); (c) Survival curve of the mice during the treatment; (d) The mass of B16F10 tumor-bearing mice during the treatment; (e) The images of the tumor tissues and (f) the average tumor mass after 12-day treatment (n=6). (* : $P \leq 0.05$; ** : $P \leq 0.01$)

4. Conclusions

In this work, PCLAMA based amphiphilic macromolecular crosslinkers were synthesized with a PEG-based hydrophilic segment, and a hydrophobic biodegradable

polyester poly(ϵ -caprolactone-co-L-lactide) segment that was end-capped with methacrylate. These crosslinkers were used for hydrogel preparation with hydrophilic monomers. It was found that hydrogels with PCLAMAs with long polyester segments or large level of PCLAMAs showed small pore sizes and swelling ratios 300-400%. Among them, the nanogels W10-2 showed high levels of 5-ALA entrapment, which allowed controlled release of drugs in responsive to the presence of lipase thus solving the problem of poor accumulation/uptake of 5-ALA in targeted cells. Here, 5-ALA loaded W10-2 nanogels improved the PDT activity when applied to skin cancer cells in vitro and tumor in vivo.

Credit authorship contribution statement

Xiao Liu: Methodology, validation, synthesis of crosslinkers and preparation of hydrogels, chemical characterization, data analysis, writing-original draft, visualization. Yuan Zhang: Synthesis and characterization, validation, data analysis and visualization. Peng Zhang: designed and carried out the in vivo experiment, data analysis and writing-original draft. Kang Ge: Methodology, validation, cell culture support. Ruzhi Zhang: Methodology, supervision. Yixin Sun: Methodology, supervision. Yang Sheng: writing-review & editing. Mark Bradley: Methodology, writing-review & editing. Rong Zhang: Conceptualization, methodology, re-sources, writing-review & editing, supervision, Project administration, funding acquisition.

Declaration of Competing Interest

The authors declare that they have no known competing financial interests or personal relationships that could have appeared to influence the work reported in this paper.

Data Availability

Data will be made available on request.

Acknowledgements

We gratefully acknowledge the support from the Jiangsu Innovative & Entrepreneurial Talent group program (2017.37), 'Six talent peaks' team

project in Jiangsu Province (SWYY-CXTD-001), International cooperation project of Changzhou City (CZ20190019) and the Priority Academic Program Development (PAPD) of Jiangsu Higher Education Institutions.

Appendix A. Supporting information

Supplementary data associated with this article can be found in the online version at: XXX.

References

- [1] J.C. Kennedy, R.H. Pottier, D.C. Pross. Photodynamic therapy with endogenous protoporphyrin IX: Basic principles and present clinical experience. *J Photoch Photobio B*, 14(1990): 275-92.
- [2] C.A. Morton, R.M. Szeimies, N. Basset-Seguín, P. Calzavara-Pinton, Y. Gilaberte, M. Haedersdal, G.F.L. Hofbauer, R.E. Hunger, S. Karrer, S. Piaserico, C. Ulrich, A.M. Wennberg, L.R. Braathen. European Dermatology Forum guidelines on topical photodynamic therapy 2019 Part 1: treatment delivery and established indications - actinic keratoses, Bowen's disease and basal cell carcinomas. *J Eur Acad Dermatol Venereol*, 33(2019): 2225-38.
- [3] A. Casas. Clinical uses of 5-aminolaevulinic acid in photodynamic treatment and photodetection of cancer: A review. *Cancer Lett*, 490(2020): 165-73.
- [4] C.M. Beddoes, C.P. Case, W.H. Briscoe. Understanding nanoparticle cellular entry: A physicochemical perspective. *Adv Colloid Interface*, 218(2015): 48-68.
- [5] S. Liu, Z.P. Liu, W. Fu. Research progress in new dosage forms of 5-aminolevulinic acid. *Progress in Biomedical Engineering*, 36(2015): 226-30.
- [6] A. Li, C. Liang, L. Xu, Y. Wang, J. Shi. Boosting 5-ALA-based photodynamic therapy by a liposomal nanomedicine through intracellular iron ion regulation. *Acta Pharm Sin B*, 11(2021): 1329-40.
- [7] D. Guimares, A. Cavaco-Paulo, E. Nogueira. Design of liposomes as drug delivery system for therapeutic applications. *Int J Pharm*, 601(2021): 120571.
- [8] Q.H. Chen. *New technology and application of drug microencapsulation*. PMPH, 2008.
- [9] L. Shi, X.L. Wang, Q.F. Tu, F. Zhao, H.S. Luan, H. Wang, H.W. Wang. Killing effect of aminolevulinic acid photodynamic therapy loaded with polyglycolide and lactide nanoparticles on A431 cells. *Chin J Derm*, 46(2013): 702-6.
- [10] X.Y. Xu, X.L. Qi, Z.H. Wu. Research progress of tumor microenvironment responsive nano gel drug delivery system. *Prog Pharm S*, (2020): 35-42.
- [11] J. Hou, T.F. Liu, C. Ge, H. Tian, T.Y. Cheng, H. Li. Silencing the expression of adipose triglyceride lipase gene inhibits the proliferation, migration and

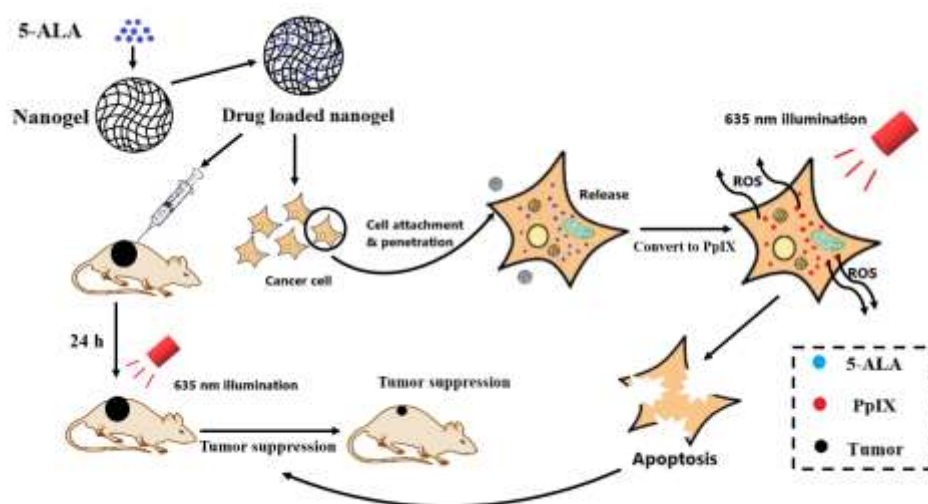
- invasion of hepatocellular carcinoma cells. *Tumor*, 37(2017): 474-82.
- [12] J. Bai. Progress in enzyme responsive hydrogels. *J Mater Sci Eng*, 35(2017): 681-8.
- [13] S. Behtaj, F. Karamali, E. Masaeli, Y.G. Anissimov, M. Rybachuk. Electrospun PGS/PCL, PLLA/PCL, PLGA/PCL and pure PCL scaffolds for retinal progenitor cell cultivation. *Biochem Eng J*, 166(2021): 107846.
- [14] M. Ponjavic, M.S. Nikolic, N. Runic, S. Jeremic, S. Stevanovic, J. Djonlagic. Degradation behaviour of PCL/PEO/PCL and PCL/PEO block copolymers under controlled hydrolytic, enzymatic and composting conditions - ScienceDirect. *Polym Test*, 57(2017): 67-77.
- [15] Y. Gao, L. Chen, L.X. Yang, C. Xu, J.P. Li. Research progress in the structure and preparation of polycaprolactone drug controlled release carriers. *Chin Polym Bull*, 9(2021): 19-30.
- [16] S.A. Munim, Z.A. Raza. Poly(lactic acid) based hydrogels: formation, characteristics and biomedical applications. *J Porous Mater*, 26(2019): 881-901.
- [17] Y. Fu, Y. Ding, L. Zhang, Y. Zhang, P. Yu. Poly Ethylene Glycol (PEG)-Related Controllable and Sustainable Antidiabetic Drug Delivery Systems. *Eur J Med Chem*, 217(2021): 113372.
- [18] M. Kurakula, G. Rao. Type of Article: REVIEW Pharmaceutical Assessment of Polyvinylpyrrolidone (PVP): As Excipient from Conventional to Controlled Delivery Systems with a Spotlight on COVID-19 Inhibition. *J Drug Deliv Sci Technol*, 60(2020): 102046.
- [19] C. You, L. Ning, H. Wu, C. Huang, F. Wang. A biocompatible and pH-responsive nanohydrogel based on cellulose nanocrystal for enhanced toxic reactive oxygen species generation. *Carbohydr Polym*, 258(2021): 117685.
- [20] G. Janarthanan, M.M. Pillai, S. Sahanand, R. Selvakumar, A. Bhattacharyya. Engineered knee meniscus construct: understanding the structure and impact of functionalization in 3D environment. *Polym Bull*, 77(2020): 2611-29.
- [21] C.A. Gang, B. Yz, A. Yx, C. Cz, D. Tl, C. Kwb. Chitosan nanoparticles for oral photothermally enhanced photodynamic therapy of colon cancer. *Int J Pharm*, 589(2020): 119763.
- [22] Y. Wang, S. Fu, Y. Lu, R. Lai, Z. Liu, W. Luo, Y. Xu. Chitosan/hyaluronan nanogels co-delivering methotrexate and 5-aminolevulinic acid: A combined chemo-photodynamic therapy for psoriasis. *Carbohydr Polym*, 277(2021): 118819.
- [23] A. Li, C. Liang, L. Xu, Y. Wang, J. Shi. Boosting 5-ALA-based photodynamic therapy by a liposomal nanomedicine through intracellular iron ion regulation. *Acta Pharmaceutica Sinica B*, 11(2021): 1329-49.
- [24] C. Zhang, X. Zhao, D. Li, F. Ji, A. Dong, X. Chen, J. Zhang, X. Wang, Y. Zhao, X. Chen. Advances in 5-aminoketovaleric acid(5-ALA) nanoparticle delivery

system based on cancer photodynamic therapy. *J Drug Deliv Sci Technol*, 78(2022): 103933.

[25] B. Gillissen, A. Richter, F. Essmann, W. Kemmner. Alectinib treatment improves photodynamic therapy in cancer cell lines of different origin. *BMC Cancer*, 21(2021): 971.

[26] Z.M. Wang, J.T. He, L. Lin. Effects of different concentrations and pH values of DFO, 5-ALA on protoporphyrin aggregation in colorectal cancer cells. *J of Hunan Normal University*, (2009): 5-8.

Graphical abstract



Credit authorship contribution statement

Xiao Liu: Methodology, validation, synthesis of crosslinkers and preparation of hydrogels, chemical characterization, data analysis, writing-original draft, visualization. Yuan Zhang: Synthesis and characterization, validation, data analysis and visualization. Peng Zhang: designed and carried out the in vivo experiment, data analysis and writing-original draft. Kang Ge: Methodology, validation, cell culture support. Ruzhi Zhang: Methodology, supervision. Yixin Sun: Methodology, supervision. Yang Sheng: writing-review & editing. Mark Bradley: Methodology,

writing-review & editing. Rong Zhang: Conceptualization, methodology, re-sources, writing-review & editing, supervision, Project administration, funding acquisition.

Declaration of interests

The authors declare that they have no known competing financial interests or personal relationships that could have appeared to influence the work reported in this paper.

The authors declare the following financial interests/personal relationships which may be considered as potential competing interests:

Highlights

- Biocompatible and biodegradable nanogel carriers loaded with 5-ALA were developed;
- Nanogels were able to deliver 5-ALA into skin cancer cells;
- Nanogels released 5-ALA more rapidly with the presence of the enzyme;
- Nanogels showed excellent photodynamic activity both *in vitro* and *in vivo*.